물리탐사
Vol. 1, No. 1, 1998, p. 8~18

Kinematic Approximation of Partial Derivative Seismogram with respect to Velocity and Density*

Shin, Changsoo[1] and Shin, Sungryul[2]

편미분 파동장을 이용한 탄성파 주시 곡선의 평가

신창수 · 신성렬

Abstract : In exploration seismology, the Kirchhoff hyperbola has been successfully used to migrate reflection seismograms. The mathematical basis of Kirchhoff hyperbola has not been clearly defined and understood for the application of prestack or poststack migration. The travel time from the scatterer in the subsurface to the receivers (exploding reflector model) on the surface can be a kinematic approximation of Green's function when the source is excited at position of the scatterer. If we add the travel time from the source to the scatterer in the subsurface to the travel time of exploding reflector model, we can view this travel time as a kinematic approximation of the partial derivative wavefield with respect to the velocity or the density in the subsurface. The summation of reflection seismogram along the Kirchhoff hyperbola can be evaluated as an inner product between the partial derivative wavefield and the field reflection seismogram. In addition to this kinematic interpretation of Kirchhoff hyperbola, when we extend this concept to shallow refraction seismic data, the stacking of refraction data along the straight line can be interpreted as a measurement of an inner product between the first arrival waveform of the partial derivative wavefield and the field refraction data. We evaluated the Kirchhoff hyperbola and the straight line for stacking the refraction data in terms of the first arrival waveform of the partial derivative wavefield with respect to the velocity or the density in the subsurface. This evaluation provides a firm and solid basis for the conventional Kirchhoff migration and the straight line stacking of the refraction data.

요 약 : 키르히호프 주시 쌍곡선은 탄성파 탐사에서 반사파 자료를 구조보정 하는데 널리 쓰여져 왔다. 그러나 이는 중합전 혹은 중합후 구조보정을 위한 적용에 있어 그 수학적인 기반이 그다지 명확하게 이해되어 오지 않아왔다. Exploding reflector 모델을 생각할 때 지하 산란체로부터 지표 수신기까지의 주시는 지하 산란체 위치에 송신원을 둔 경우 Green 함수를 이용한 주시와 동일하다. 따라서 송신원에서 exploding reflector, 또 여기서 수신기까지의 주시의 합은 관측자료에 속도 및 밀도에 대한 편미분을 취함으로써 얻어지는 편미분 파동장의 주시와 개념적으로 일치한다. 키르히호프의 주시 쌍곡선을 따라 반사파 탄성파자료의 합은 편미분장과 관측된 자료의 내적과 동일한 것으로 간주될 수 있다. 또한 굴절 주시 직선을 이용한 굴절자료의 중합은 편미분장의 초동과 현장자료의 내적과 개념적으로 같음을 알 수 있다. 지하의 구조내의 속도나 밀도에 대한 편미분장의 관점에서 보면 굴절파자료에 대해서는 직선에 대한 중합, 반사파자료에 대해서는 키르히호프 쌍곡선으로 지하의 구조를 영상화 할 수 있는 연산자임을 확인하였다. 이러한 타당성 검증은 일반적인 키르히호프 구조보정에 대한 기본 이론을 구성할 수 있었고 또한 굴절 주시 직선을 굴절파 자료의 영상화에 있어서 연산자의 기본 지식을 확보할 수 있었다.

Keywords : Partial derivative seismogram, Kinematic approximation, Virtual Source, Kirchhoff hyperbola, Cross-correlation

Introduction

Exploration geophysicists use prestack depth migration using ray tracing technique to image the subsurface. The travel time curve calculated by ray tracing using source and receiver reciprocity can be thought of as a kinematic approximation of the partial derivative seismogram with respect to velocity or density. The scattering wave field by Gardner, *et al.* (1974) and the Born perturbation seismogram by Bleistein, *et al.* (1985) can be approximated kinematically by the travel time curve from the source to scatterer, and then, to the receiver. These scattering wave field and the Born perturbation seismogram are closely related to the partial derivative seismogram with respect to velocity and density, which was applied to the waveform inversion (Shin, 1988).

The computation of the partial derivative seismogram by numerical modeling techniques such as the finite ele-

*1998년 5월 1일 접수

1) Seoul Nat'l Univ. School of Civil Urban & Geosystem Eng.
2) Ssangyong Engineering & Construction Co. Ltd., Institute of Construction Technology

ment method and the finite difference method is a formidable task unless one uses the source and receiver reciprocity for the computation of Green function and the partial derivative seismogram. The computation of the partial derivative seismogram by numerical modeling technique involves three steps. The first step is the calculation of the numerical Green function by exciting the source on the surface of the internal point of the geologic model. The next step is the computation of the virtual source required to calculate the partial derivative seismogram. The third step is the convolution of the virtual source with the Green function. In this way, one can compute the partial derivative seismogram. However, this approach is extremely expensive, impractical and beyond the capability of modern computers. Alternative to this is the exploitation of the source and receiver reciprocity for the computation of the partial derivative seismogram. The applications of the source and receiver reciprocity can be divided into three categories. One is the kinematic approximation of the partial derivative seismogram using the ray tracing.

The second approach is the use of Claerbout's one way wave equation, which results in the weighted hyperbola having the amplitude and phase change along the travel time curve. In this case, we are not using the entire wave events of the partial derivative seismogram as generated by full waveform modeling technique. The third approach, although most expensive, is the employing of the finite difference method or the finite element modeling technique using the source and receiver reciprocity, which is not discussed fully in this paper.

In this paper, we present the wave theoretical support for the kinematic approximation of the partial derivative seismogram using various numerical modeling techniques including ray tracing by exploiting the source and reciprocity. As with the kinematic approximation of the partial derivative seismogram for the reflection seismogram, we analyzed the kinematic evaluation of the partial derivative seismogram for the shallow refraction seismogram stacking initiated by Landa *et al.* (1993) and the mathematical aspect of the imaging subsurface using the partial derivative seismogram.

Partial Derivative Seismograms with Respect to the Material Parameter

In a two dimensional medium, the acoustic wave equation is given by

$$\frac{\partial}{\partial x}\left(k\frac{\partial U}{\partial x}\right)+\frac{\partial}{\partial x}\left(k\frac{\partial U}{\partial z}\right)-\rho\frac{\partial^2 U}{\partial t^2}=f(x,z,t). \tag{1}$$

Where, x is the horizontal distance, z is the depth, t is time, $U(x, z, t)$ is the displacement wave field, $\rho(x, z)$ is density, $k(x, z)$ is bulk modulus, and $f(x, z, t)$ is the source function.

Many numerical modeling techniques are available in solving the equation. For simplicity in evaluating the principle of the partial derivative seismogram, we use a discrete notation of the time domain finite difference technique, fix the bulk modulus and perturb the density parameter. Figure 1 shows the discretized domain, in which finite difference expression of Eq. (1), without any boundary condition to suppress the artificial reflection, can be given as

$$\frac{1}{\Delta t^2}\begin{pmatrix}\rho^1 u_1^{j+1}\\ \cdot\\ \cdot\\ \rho^i u_i^{j+1}\\ \cdot\\ \cdot\\ \rho^n u_n^{j+1}\end{pmatrix}=\frac{2}{\Delta t^2}\begin{pmatrix}\rho^1 u_1^{j}\\ \cdot\\ \cdot\\ \rho^i u_i^{j}\\ \cdot\\ \cdot\\ \rho^n u_n^{j}\end{pmatrix}-\frac{1}{\Delta t^2}\begin{pmatrix}\rho^1 u_1^{j-1}\\ \cdot\\ \cdot\\ \rho^i u_i^{j-1}\\ \cdot\\ \cdot\\ \rho^n u_n^{j-1}\end{pmatrix} \tag{2}$$

$$-\frac{1}{\Delta^2}\begin{pmatrix}
-4k_1 & k_1 & 0 & \cdot & \cdot & k_1 & 0 & \cdot & \cdot & \cdot & \cdot & \cdot & \cdot\\
k_2 & -4k_2 & k_2 & 0 & \cdot & \cdot & k_2 & 0 & \cdot & \cdot & \cdot & \cdot & \cdot\\
0 & k_3 & -4k_3 & k_3 & 0 & \cdot & \cdot & k_3 & 0 & \cdot & \cdot & \cdot & \cdot\\
\cdot & 0 & \cdot & \cdot & \cdot & 0 & \cdot & \cdot & \cdot & 0 & \cdot & \cdot & \cdot\\
\cdot & 0 & 0 & \cdot & \cdot & \cdot & 0 & \cdot & \cdot & \cdot & 0 & \cdot & \cdot\\
\cdot & \cdot & 0 & 0 & \cdot & \cdot & \cdot & 0 & \cdot & \cdot & \cdot & 0 & \cdot\\
k_i & \cdot & \cdot & 0 & 0 & k_i & -4k_i & k_i & 0 & \cdot & \cdot & k_i & 0\\
0 & \cdot & \cdot & \cdot & 0 & 0 & \cdot & \cdot & \cdot & 0 & \cdot & \cdot & \cdot\\
\cdot & 0 & \cdot & \cdot & \cdot & 0 & 0 & \cdot & \cdot & \cdot & 0 & \cdot & \cdot\\
\cdot & \cdot & 0 & \cdot & \cdot & \cdot & 0 & 0 & \cdot & \cdot & \cdot & 0 & \cdot\\
\cdot & \cdot & \cdot & 0 & \cdot & \cdot & \cdot & 0 & 0 & \cdot & \cdot & \cdot & 0\\
\cdot & \cdot & \cdot & \cdot & 0 & \cdot & \cdot & \cdot & 0 & 0 & \cdot & \cdot & \cdot\\
\cdot & \cdot & \cdot & \cdot & \cdot & 0 & k_n & \cdot & \cdot & 0 & 0 & k_n & -4k_n
\end{pmatrix}$$

$$\begin{pmatrix}u_1^j\\ \cdot\\ \cdot\\ u_i^j\\ \cdot\\ \cdot\\ u_n^j\end{pmatrix}=\begin{pmatrix}f_1^j\\ \cdot\\ \cdot\\ f_1^j\\ \cdot\\ \cdot\\ f_n^j\end{pmatrix}$$

where j is the index for discrete time, i for discrete x-axis and z-axis, dt is the grid step in time, and Δ is the grid step for x-axis and z-axis. Due to the difficulty denoting the matrix notation of Laplacian term, we did not put zeroes at some elements of the super diagonal and the sub diagonal of the matrix in Eq. (2) due to the finite size of the model.

Taking the derivative of Eq. (2) with respect to the ith density yields

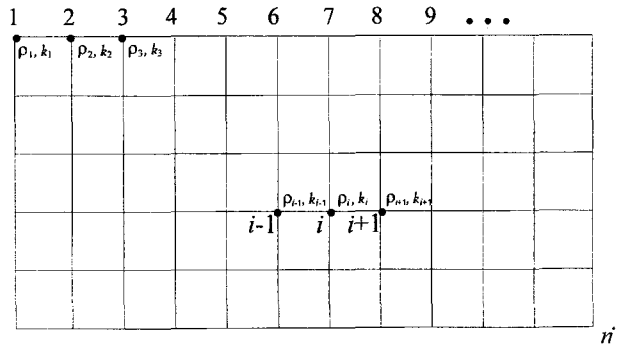

Fig. 1. A discrete representation of the finite difference forward modeling for acoustic wave equation. The bulk modulus and density of each nodal point is parameterized to compute the partial derivative seismogram.

$$\frac{1}{\Delta t^2}\begin{pmatrix} \rho^1 \dfrac{\partial u_1^{j+1}}{\partial \rho^1} \\ \cdot \\ \cdot \\ \rho^i \dfrac{\partial u_i^{j+1}}{\partial \rho^i} \\ \cdot \\ \cdot \\ \rho^n \dfrac{\partial u_n^{j+1}}{\partial \rho^n} \end{pmatrix} - \frac{2}{\Delta t^2}\begin{pmatrix} \rho^1 \dfrac{\partial u_1^{j}}{\partial \rho^i} \\ \cdot \\ \cdot \\ \rho^i \dfrac{\partial u_i^{j}}{\partial \rho^i} \\ \cdot \\ \cdot \\ \rho^n \dfrac{\partial u_n^{j}}{\partial \rho^n} \end{pmatrix} + \frac{1}{\Delta t^2}\begin{pmatrix} \rho^1 \dfrac{\partial u_1^{j-1}}{\partial \rho^1} \\ \cdot \\ \cdot \\ \rho^i \dfrac{\partial u_i^{j-1}}{\partial \rho^i} \\ \cdot \\ \cdot \\ \rho^n \dfrac{\partial u_n^{j-1}}{\partial \rho^n} \end{pmatrix} \tag{3}$$

$$-\frac{1}{\Delta^2}\begin{pmatrix} -4k_1 & k_1 & 0 & \cdots & k_1 & 0 & \cdots & \cdots & \cdots \\ \cdot & k_2 & -4k_2 & k_2 & 0 & \cdots & k_2 & 0 & \cdots \\ \cdot & 0 & k_3 & \cdots & k_3 & 0 & \cdots & k_3 & 0 \\ \cdot & \cdot & 0 & \cdots & \cdots & 0 & \cdots & \cdots & 0 \\ \cdot & \cdot & 0 & 0 & \cdots & \cdots & 0 & \cdots & \cdots \\ \cdot & \cdot & \cdot & 0 & 0 & \cdots & \cdots & 0 & \cdots \\ \cdot & k_i & \cdot & \cdot & 0 & 0 & k_i & k_i & 0 \\ 0 & 0 & \cdot & \cdot & \cdot & 0 & 0 & \cdots & \cdots \\ \cdot & \cdot & 0 & \cdots & \cdots & 0 & 0 & \cdots & \cdots \\ \cdot & \cdot & \cdot & 0 & \cdots & \cdots & 0 & 0 & \cdots \\ \cdot & \cdot & \cdot & \cdot & 0 & \cdots & \cdots & 0 & 0 \\ 0 & \cdot & \cdot & \cdot & \cdot & 0 & \cdots & \cdots & 0 \\ \cdot & \cdot & \cdot & \cdot & \cdot & \cdot & 0 & k_n & \cdots \end{pmatrix}$$

$$\begin{pmatrix} 0 & \cdots & \cdots \\ \cdot & & \\ \cdot & & \\ 0 & 0 & 0 \\ \cdot & & \\ \cdot & & \\ 0 & \cdots & \cdots \\ \cdot & & \\ \cdot & & \\ 0 & \cdots & \cdots \\ \cdot & & \\ \cdot & & \\ 0 & k_n & \cdots \end{pmatrix} \begin{pmatrix} 0 & \cdots & \cdots \\ \cdot & & \\ \cdot & & \\ 0 & 0 & 0 \\ \cdot & & \\ \cdot & & \\ 0 & \cdots & \cdots \\ \cdot & & \\ \cdot & & \\ 0 & \cdots & \cdots \\ \cdot & & \\ \cdot & & \\ 0 & k_n & \cdots \end{pmatrix}$$

$$\begin{pmatrix} \dfrac{\partial u_1^j}{\partial \rho^i} \\ \cdot \\ \cdot \\ \dfrac{\partial u_i^j}{\partial \rho^i} \\ \cdot \\ \cdot \\ \dfrac{\partial u_n^j}{\partial \rho^n} \end{pmatrix} = \begin{pmatrix} f_1^{j*} \\ \cdot \\ \cdot \\ f_i^{j*} \\ \cdot \\ \cdot \\ f_n^{j*} \end{pmatrix}$$

where the right most column vector of Eq. (3) can be given as

$$\begin{pmatrix} f_1^{j*} \\ \cdot \\ \cdot \\ f_i^{j*} \\ \cdot \\ \cdot \\ f_n^{j*} \end{pmatrix} = -\frac{1}{\Delta t^2}\begin{pmatrix} 0 \\ \cdot \\ \cdot \\ u_i^{j+1} - 2u_i^j + u_i^{j-1} \\ \cdot \\ \cdot \\ 0 \end{pmatrix} \tag{4}$$

and $\partial u_i^j / \partial \rho^i$ is the partial derivative of the displacement field with respect to the i th density parameter.

We will refer to f_i^* in Eq. (3) and (4) as a virtual source or an actual source to compute the partial derivative wave field. It is critical to examine the physical meaning of the virtual source. In computing the partial derivative seismogram using Eq. (3), one has to catch the wave field that passes through the *i*th nodal point and save it for the computation of the partial derivative seismogram. Note that when perturbing the density parameter at the *i*th nodal point, the virtual source has numerical support at the *i*th nodal point. We would like to put special emphasis on the virtual source. The virtual source when perturbing the bulk modulus parameter, can be the extra acceleration generated by the primary wave field (the source generated wave field) at the *i*th nodal point. In other words, the virtual source is the force by Newton's second law (*F=ma*). In this case, the virtual source is the force given by the multiplication of acceleration with the unit mass (Note that in the usual expression of the acoustic wave equation the density can be replaced by the bulk modulus parameter in Eq. (1), (2) and (3)). The best account for this scattering or perturbation can be found in the text book by Officer (1958).

Figure 3 shows the virtual source at the *i*th nodal point when perturbing the density parameter of the *i*th nodal points as shown in Figure 2. When we consider the first arrival part of the virtual source in Figure 3, we can approximately express the virtual source without the amplitude and the later arrival events as

$$f_i(t)^* \cong \delta(t - t_i^k) \tag{5}$$

where δ is the delta function, i denotes the *i*th nodal point, t is the time, and t_i^k is the first arrival time from the *k*th source point to the *i*th nodal point. There are two ways to compute the partial derivative seismogram. One is by using the virtual source as a source function in Eq. (2). We will refer to this approach as the brute approach, which is extremely expensive and beyond the capability of modern computers for multiple shots problems (for example, sup-

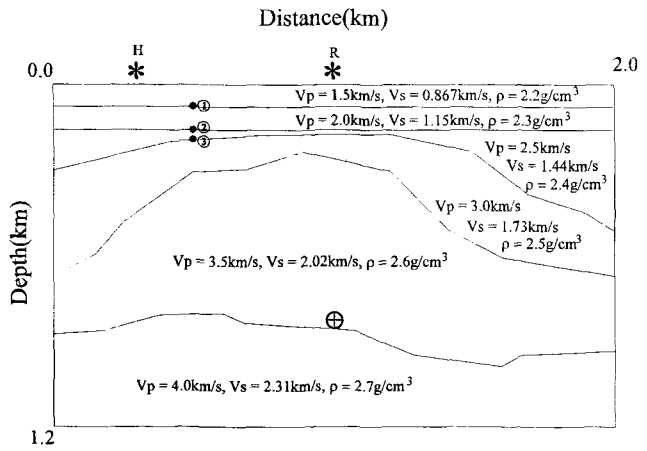

Fig. 2. A geologic model taken to compute the partial derivative seismogram with respect to the velocity and the density. Symbol+ denotes the point to be perturbed. Symbol 1, 2, and 3 are the points to be perturbed for the computation of the partial derivative seismogram for the head waves.

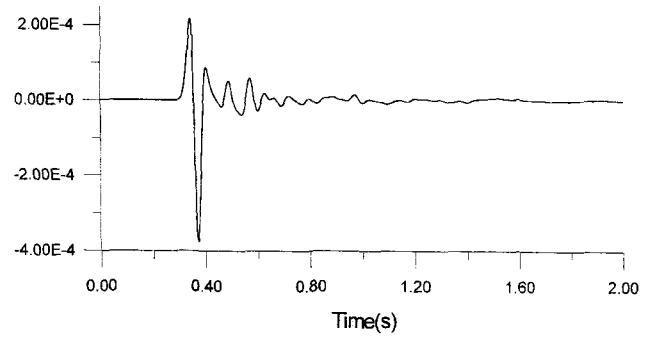

Fig. 3. The virtual source function when perturbing the density point indicated by symbol+in Figure 2.

pose the geologic model is subdivided into nx by nz grids and one wants to calculate the partial derivative seismogram with respect to each grid parameter for multiple shots, one needs to do the forward modeling ns × nx × nz times, where nx is the number of grid points, nz is the number of grid points). We use the brute approach not for the future application that can assist in imaging the subsurface, but for a clear visualization of the partial derivative seismogram. Figure 4 shows the partial derivative seismogram with respect to the *i*th density parameter when we used the virtual source shown in Figure 3 as a source function.

The other approach is the direct convolution between the virtual source and the Green function, which is less expensive than the brute approach but still requires a massive computation of the Green function. We would like to discuss it a little more before moving on to the kinematic approximation of the partial derivatives seismogram. Figure 5 shows the Green function shown in Figure 5, the kinematic waveform expression of the Green function can

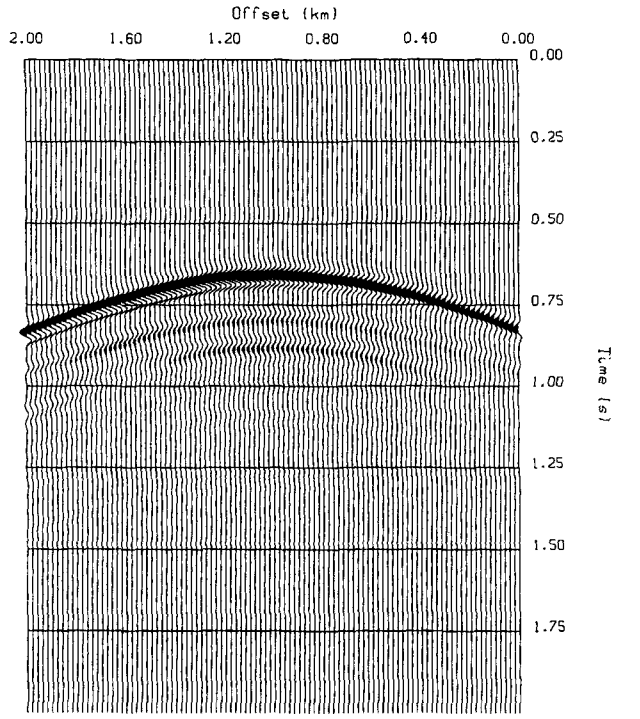

Fig. 4. A partial derivative seismogram with respect to the density of the point shown in Figure 2.

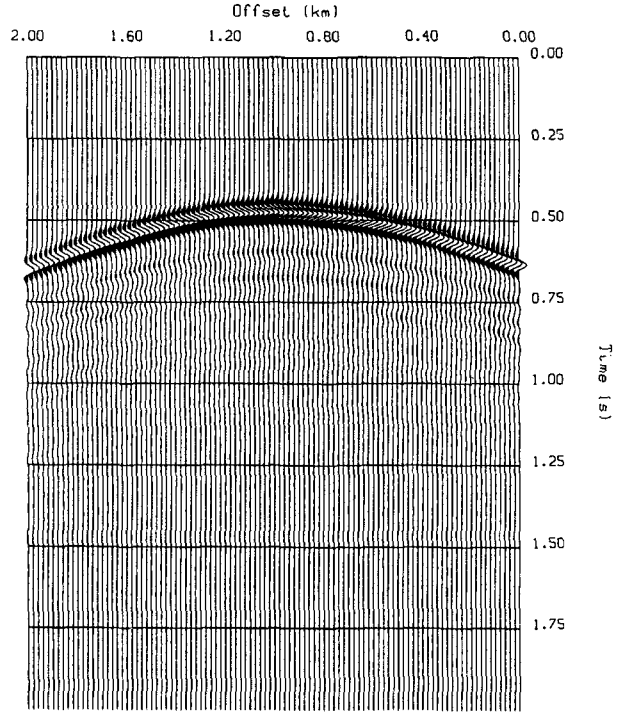

Fig. 5. Green function calculated at the surface using the finite difference forward modeling.

be given as

$$G(x, z=0, t) = \delta(t - t_k^i), k = 1, \cdots, m \quad (6)$$

where x is the horizontal distance in the x direction, z is

the distance in the z direction, t is the time, k is the receiver nodal index at the surface, and t_k^i is the travel time from the ith nodal point to the surface receivers. By convolving the virtual source in Figure (3) with the Green function in Figure 5, we can obtain the partial derivative seismogram as calculated by the brute approach. In practicing this type approach, since the impulse response (Green function) and the virtual source are convolved with the source wavelet, we have to deconvolve the impulse response and the virtual source and convolve them again. In this regard, the frequency domain modeling technique of Marfurt (1984), Pratt and Worthington (1990), Jo *et al.* (1996), and Shin and Sohn (1997) is more flexible than the time domain modeling technique.

Figure 6 shows the partial derivative seismogram computed by the convolution of the Green function with the virtual source. Based on this discussion, it is straight forward to approximate the kinematic waveform of the partial derivative seismogram using the ray tracing technique. For simplicity in giving an aid to the visualization of the Green function, we use simple shooting ray tracing. As shown in Figure 7, we shoot the rays into the general directions at the i the nodal point and calculate the travel time from the ith nodal point to the receivers. In this case, the waveform expression of the travel time can be given as shown in Eq. (6). Figure 8 shows the waveform of the travel time calculated by shooting ray tracing. From Figure 5 and 8, we cannot tell the difference of the first arrival time between the partial derivative seismogram approximated by ray tracing and the partial derivative seismogram computed by the finite difference modeling technique. The next step is to calculate the travel time from the kth source point to the ith nodal point, which is equivalent to the first arrival time of the virtual source. If we limit and confine our attention to the kinematics of the partial derivative seismogram, we can exploit the source and receiver reciprocity. The simple mathematical expression can be given as

$$\frac{\partial u}{\partial \rho^i} = \delta(t - t_i^k) * \delta(t - t_k^i) \tag{7a}$$

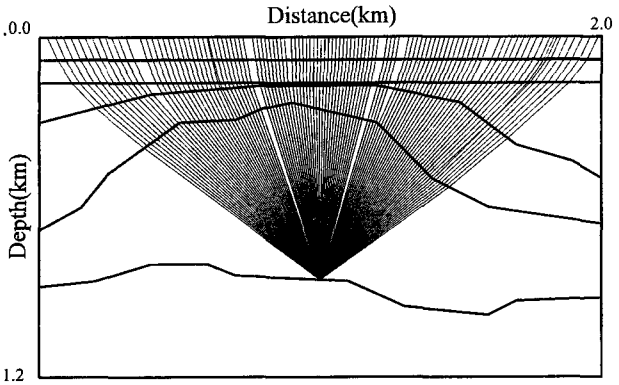

Fig. 7. The ray diagram when one shoots the rays at the point to be perturbed in Figure 2 into the upward direction.

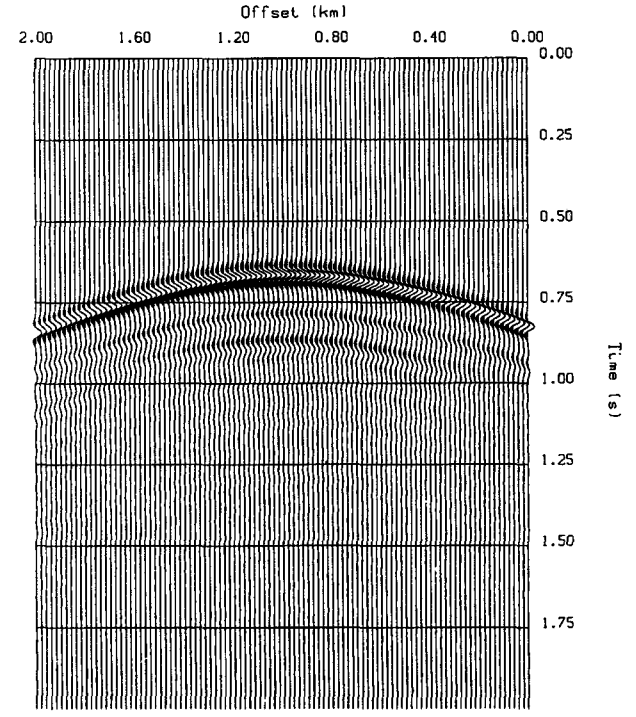

Fig. 6. A partial derivative seismogram computed by convolving the virtual source function in Figure 3 with Green function in Figure 5.

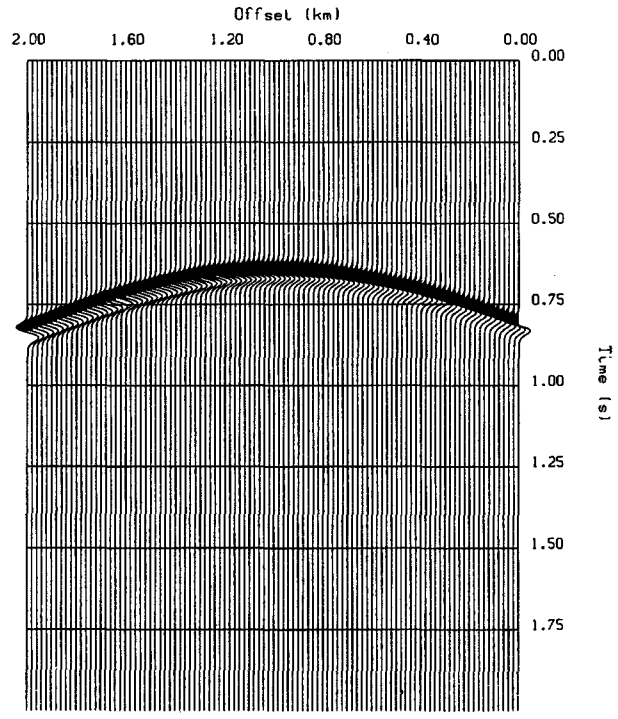

Fig. 8. The kinematic approximation of the partial derivative seismogram in Figure 4 using ray tracing.

or

$$\frac{\partial u}{\partial \rho^i} = \delta(t - t_i^k - t_k^i) \tag{7b}$$

where * denotes the convolution. Figure 8 shows the kinematic waveform expression calculated by Eq. (7b). As we see in the Green function by the finite difference modeling and ray tracing, the first arrival events of Figure 4 and 8 have the same travel time. Before going into the details of this approach, we should mention the efficiency of this ray tracing approach.

Suppose that the geologic model to be imaged can be divided into the nx by nz discrete grid points, where nx is the number of grid points into the x direction and nz is the number of grid points into z direction. In this case, we have to calculate the travel time nx by nz times. This approach is not economical except for the advantage that we can make the weighted Kirchhoff hyperbola due to the geometrical spreading and the change in the reflection coefficient.

Another approach widely employed by the oil industry is using ray tracing for the kinematic approximation of the partial derivative seismogram with a slightly different source and receiver reciprocity. Instead of shooting the ray at the internal nodal point, one shoots the rays at the surface receiver points and calculates the travel time at the internal nodal point, interpolates the travel time at the point where the ray does not pass through, and computes the travel time of the first arrival of the partial derivative seismogram using the source and receiver reciprocity. This approach is extremely fast and economical compared to the approach discussed above, being the dominant technique employed by exploration seismologists.

Until now we have discussed the partial derivative seismogram with respect to the density parameter, but now, we will take a closer look at the partial derivative seismogram with respect to the bulk modulus parameter. When returning to Eq. (2), taking partial derivative of Eq. (2) with respect to the i th bulk modulus parameter yields

$$\frac{1}{\Delta t^2}\begin{pmatrix} \rho^1 \dfrac{\partial u_1^{j+1}}{\partial k^1} \\ \cdot \\ \cdot \\ \rho^i \dfrac{\partial u_i^{j+1}}{\partial k^i} \\ \cdot \\ \cdot \\ \rho^n \dfrac{\partial u_n^{j+1}}{\partial k^n} \end{pmatrix} = \frac{2}{\Delta t^2}\begin{pmatrix} \rho^1 \dfrac{\partial u_1^{j}}{\partial k^i} \\ \cdot \\ \cdot \\ \rho^i \dfrac{\partial u_i^{j}}{\partial k^i} \\ \cdot \\ \cdot \\ \rho^n \dfrac{\partial u_n^{j}}{\partial k^n} \end{pmatrix} - \frac{1}{\Delta t^2}\begin{pmatrix} \rho^1 \dfrac{\partial u_1^{j-1}}{\partial k^1} \\ \cdot \\ \cdot \\ \rho^i \dfrac{\partial u_i^{j-1}}{\partial k^i} \\ \cdot \\ \cdot \\ \rho^n \dfrac{\partial u_n^{j-1}}{\partial k^n} \end{pmatrix} \tag{8}$$

$$+\frac{1}{\Delta^2}\begin{pmatrix} -4k_1 & k_1 & 0 & \cdots & k_1 & 0 & \cdots & & \\ k_2 & -4k_2 & k_2 & 0 & \cdots & k_2 & 0 & \cdots & \\ 0 & k_3 & -4k_3 & k_3 & 0 & \cdots & k_3 & 0 & \cdots \\ \cdot & 0 & \cdots & & 0 & \cdots & & 0 & \cdots \\ \cdot & 0 & 0 & \cdots & 0 & \cdots & 0 & \cdots & \\ \cdot & \cdot & 0 & 0 & \cdots & 0 & \cdots & 0 & \cdots \\ k_i & \cdot & \cdot & 0 & 0 & k_i & -4k_i & k_i & 0 \\ 0 & \cdot & \cdot & \cdot & 0 & 0 & \cdots & 0 & \cdots \\ \cdot & 0 & \cdots & & 0 & 0 & \cdots & 0 & \cdots \\ \cdot & \cdot & 0 & \cdots & 0 & 0 & \cdots & 0 & \cdots \\ \cdot & \cdot & \cdot & 0 & \cdots & 0 & 0 & \cdots & \cdots \\ \cdot & \cdot & \cdot & \cdot & 0 & \cdots & 0 & 0 & \cdots \\ \cdot & \cdot & \cdot & \cdot & 0 & k_n & \cdots & 0 & 0 \end{pmatrix} \begin{pmatrix} \dfrac{\partial u_1^j}{\partial k^i} \\ \cdot \\ \cdot \\ \dfrac{\partial u_i^j}{\partial k^i} \\ \cdot \\ \cdot \\ \dfrac{\partial u_n^j}{\partial k^n} \end{pmatrix} = \begin{pmatrix} f_1^{j*} \\ \cdot \\ \cdot \\ f_i^{j*} \\ \cdot \\ \cdot \\ f_n^{j*} \end{pmatrix}$$

where the right most column vector of Eq. (8) can be given as

$$\begin{pmatrix} f_1^{j*} \\ \cdot \\ \cdot \\ f_i^{j*} \\ \cdot \\ \cdot \\ f_n^{j*} \end{pmatrix} = \frac{1}{\Delta^2} k_i \begin{pmatrix} 0 & 0 & 0 & \cdots & 0 & 0 & \cdots & & \\ 0 & 0 & 0 & 0 & \cdots & 0 & 0 & \cdots & \\ 0 & 0 & 0 & 0 & 0 & \cdots & 0 & 0 & \cdots \\ \cdot & 0 & 0 & 0 & 0 & 0 & \cdots & 0 & 0 \\ \cdot & \cdot & 0 & 0 & 0 & 0 & 0 & \cdots & 0 \\ \cdot & \cdot & \cdot & 0 & 0 & 0 & 0 & 0 & \cdots \\ 1 & \cdot & \cdots & 0 & 1 & -4 & 1 & 0 & \cdots \\ 0 & 0 & \cdot & \cdots & 0 & 0 & 0 & 0 & 0 \\ \cdot & 0 & 0 & \cdot & \cdots & 0 & 0 & 0 & 0 \\ \cdot & \cdot & 0 & 0 & \cdots & 0 & 0 & 0 & 0 \\ \cdot & \cdot & \cdot & 0 & 0 & \cdots & 0 & 0 & 0 \\ \cdot & \cdot & \cdot & \cdot & 0 & 0 & \cdots & 0 & 0 \end{pmatrix} \begin{pmatrix} u_1^j \\ \cdot \\ \cdot \\ u_i^j \\ \cdot \\ \cdot \\ u_n^j \end{pmatrix}$$

and $\partial u_i^j / \partial k^i$ is the partial derivative wave field with respect to the ith bulk modulus parameter.

As discussed above, the virtual source when perturbing the bulk modulus parameter is the extra dilatation force excited by the source generated primary waves. Figure 9 shows a partial derivative seismogram with respect to the bulk modulus parameter of the ith nodal point. It is clear to note that we cannot tell the difference between the partial derivative seismogram with respect to the density parameter and that of bulk modulus when we consider the first arrival events. This is the main reason why one obtains the superimposed image of the subsurface when using the kinematics of the partial derivatives seismogram. In principle, we must use the weighted Kirchhoff hy-

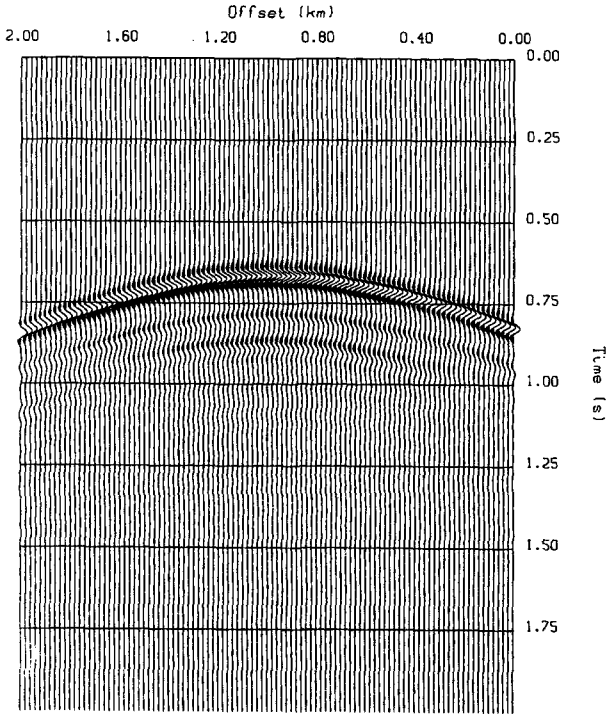

Fig. 9. A partial derivative seismogram with respect to the bulk modulus parameter of the point denoted by symbol+in Figure 2. The difference between the partial derivative seismogram with respect to the density and the partial derivative seismogram with respect to the bulk modulus parameter is the phase shift of the seismograms.

perbola shown in Figure 4 for the image of the density profile and use the weighted Kirchhoff hyperbola shown in Figure 9 for the image of the bulk modulus profile. The use of the different weighted Kirchhoff hyperbola results in a separate image of the subsurface, which is equivalent to the seismic inverse problem. A more important reason why this Kirchhoff hyperbola calculated by ray tracing is successful in imaging the subsurface for the elastic seismogram can be explained by extending the kinematic concept of the partial derivative seismogram to the elastic wave equation. Without using the discrete finite difference representation as we did in the acoustic wave equation, we can visualize the virtual source generated by the primary wave field. The source generated wave field of elastic waves can be different, depending upon the source mechanism. The ideal dynamite explosion in the subsurface is considered to generate pure P-waves. The virtual source defined by the finite difference elastic wave equation will catch the fastest arrival event.

The kinematic approximation of the resulting partial derivative seismograms with respect to the density, the P-wave velocity and the S-wave velocity is identical to each other. Figure 10 shows the partial derivative seismograms with respect to the density, the P-wave velocity, and the S-wave velocity of the ith nodal point. Except for the case of the source mechanism generating the pure S-waves, the kinematic approximation of the partial derivative seismogram of the elastic waves will be the same as of the acoustic wave equation. From the discussions above, we stress that the imaging of the surface is the use of the kinematic approximation of the partial derivative seismogram with respect to the density, the P-wave velocity and the S-wave velocity, This hyperbola can be applied to image the field seismogram for any possible source and receiver configuration including the common shot gather and the common midpoint gather configuration.

Kinematic Approximation of Partial Derivative Seismogram for Head Waves

Until now, we have discussed the use of partial derivative seismograms to image reflection seismograms, Let us move our principle on to the use of the kinematic approximation of the partial derivative seismogram for the shallow refraction survey. Considering refracted wave traveltime of two layered media case shown in Figure 2, it can be given as

$$H(x, z=0, t)=H(x_{cross}-x)\,\frac{\delta(t-x)}{v^1}$$
$$+H(x-x_{cross})\,\delta\left(t-\frac{x-2z\tan i_c}{v^2}\right) \tag{9}$$

where x is the distance in the x direction, z is the distance in the z direction x_{cross} is the crossover distance, δ is the Dirac delta function, i_c is the critical angle, v^1 is the velocity of the first layer, v^2 is the velocity of the second layer, and H is the Heaviside step function. Another expression of Eq. (9) using the discrete coordinates shown in Figure 11 can be given as

$$H(x_r, z=0, t)=AH(x_{cross}-x)\,\delta(t-t_o)$$
$$+BH(x-x_{cross})\,\delta(t-t^1-t^2-t^3) \tag{10}$$

The travel time from the source point to the surface receiver point can be given as

$$t_o=\sqrt{\frac{(x_r-x_s)^2+(z_r-z_s)^2}{v_1}} \tag{11}$$

where x_s and z_s are the coordinates of the source, respectively, x_r and z_r are the coordinates of the receiver, respectively. The travel time from the source point to the critical point can be given as

$$t_1=\sqrt{\frac{(x_c-x_s)^2+(z_c-z_s)^2}{v_1}} \tag{12}$$

where x_c and z_c are the coordinates of the critical point,

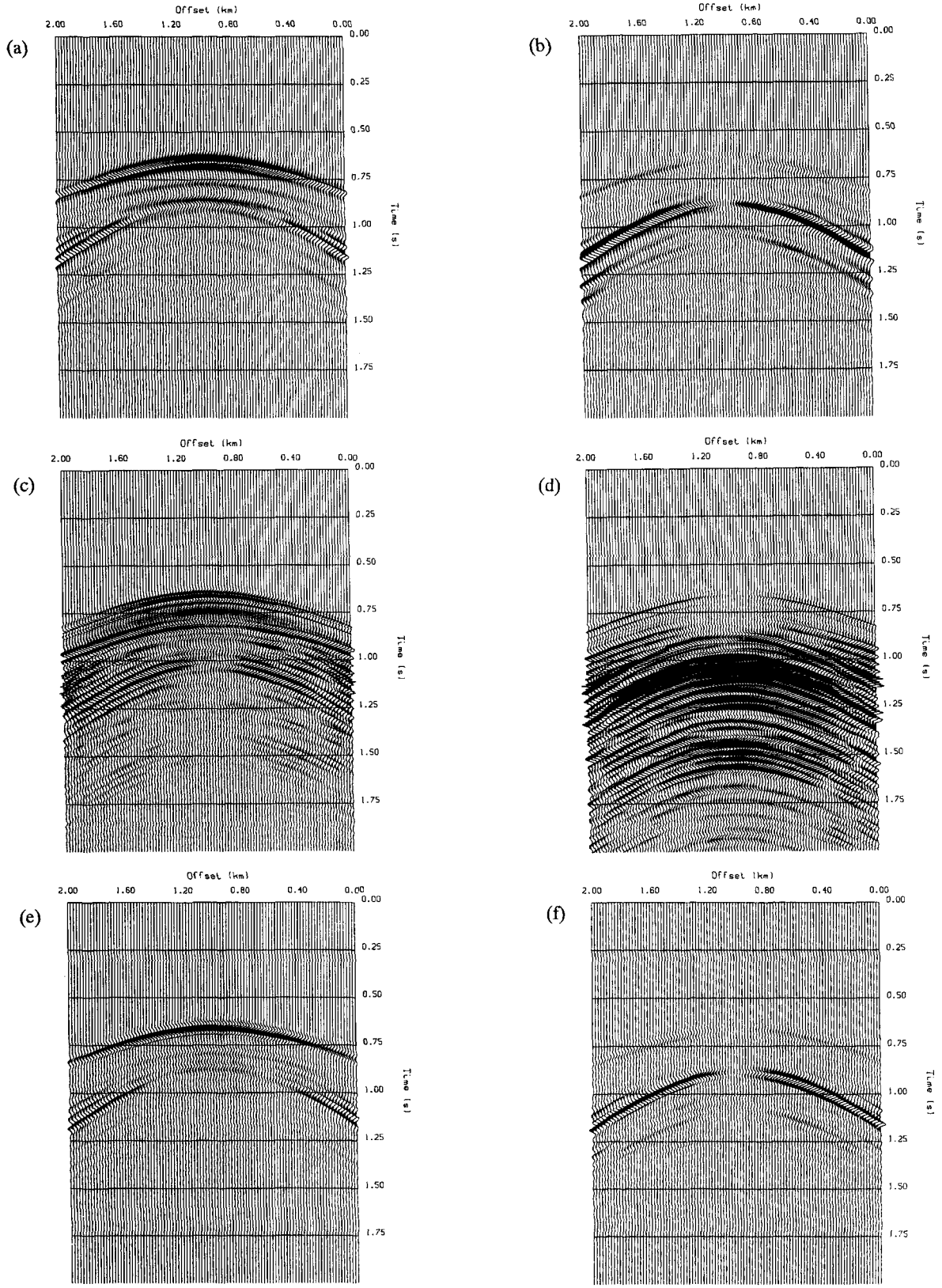

Fig. 10(a). A vertical motion of partial derivative seismogram with respect to the p wave velocity of the point in Figure 2(b) A horizontal motion of partial derivative seismogram with respect to the p wave velocity of the point in Figure 2(c) A vertical motion of partial derivative seismogram with respect to the s wave velocity of the point in Figure 2(d) A horizontal motion of a partial derivative seismogram with respect to the s wave velocity of the point in Figure 2(e) A vertical motion of partial derivative seismogram with respect to the density of the point in Figure 2(f) A horizontal motion of a partial derivative seismogram with respect to the density of the point in Figure 2.

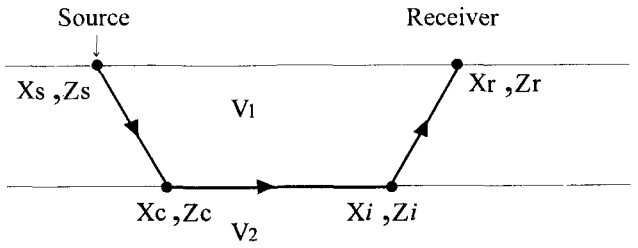

Fig. 11. A discretized coordinate of the two layered media shown in Figure 2.

respectively. The travel time from the critical point to the interface point can be given as

$$t_2 = \sqrt{\frac{(x_c - x_i)^2 + (z_c - z_i)^2}{v_2}} \tag{13}$$

where x_i and z_i are the coordinates of the interface point, respectively. The travel time from the interface point to the surface receiver can be given as

$$t_3 = \sqrt{\frac{(x_r - x_i)^2 + (z_r - z_i)^2}{v_1}} \tag{14}$$

Taking the derivative of Eq. (10) with respect to the z coordinate of the critical point yields

$$\frac{\partial H(x, z=0, t)}{\partial z^c} = B'H\,(x - x_{cross})\,\delta(t - t^1 - t^2 - t^3)$$
$$-BH\,(x - x_{cross})\,\frac{\partial (t^1 + t^2)}{\partial z^c}\,\delta'(t - t^1 - t^2 - t^3) \tag{15}$$

where B' is the derivative of B with respect to z^c, and δ' is the derivative of the delta function. The kinematic expression of Eq. (15) is a straight line, which is shown in Figure 12. Returning to equation (2) and taking the derivative of equation (2) with respect to the z coordinate of the critical point (strictly speaking, the partial derivative seismogram with respect to the interface coordinate can only be computed by the finite element modeling technique, see Shin (1988)) or by taking the derivative with respect to the velocity or density near the interface, we can have a different kinematic view of the partial derivative seismogram for seismograms.

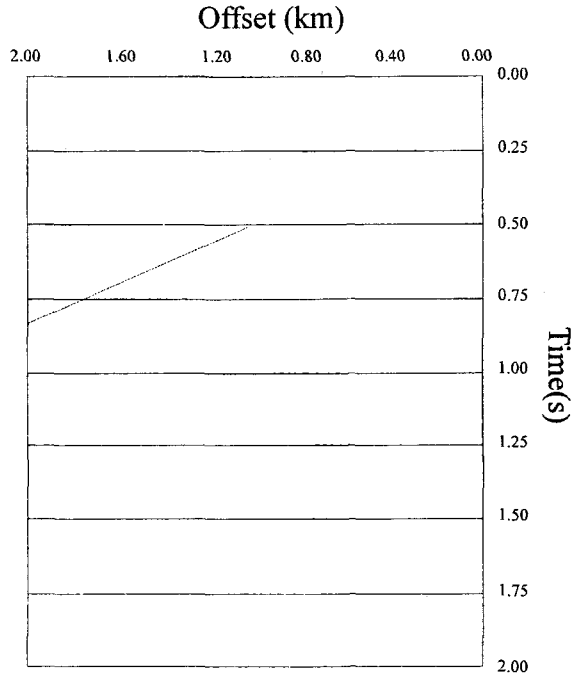

Fig. 12. A kinematic expression of the partial derivative seismogram with respect to the critical point shown in Figure 11.

Figure 13 shows the partial derivative seismogram with respect to the velocity of the nodal points in Figure 2. If

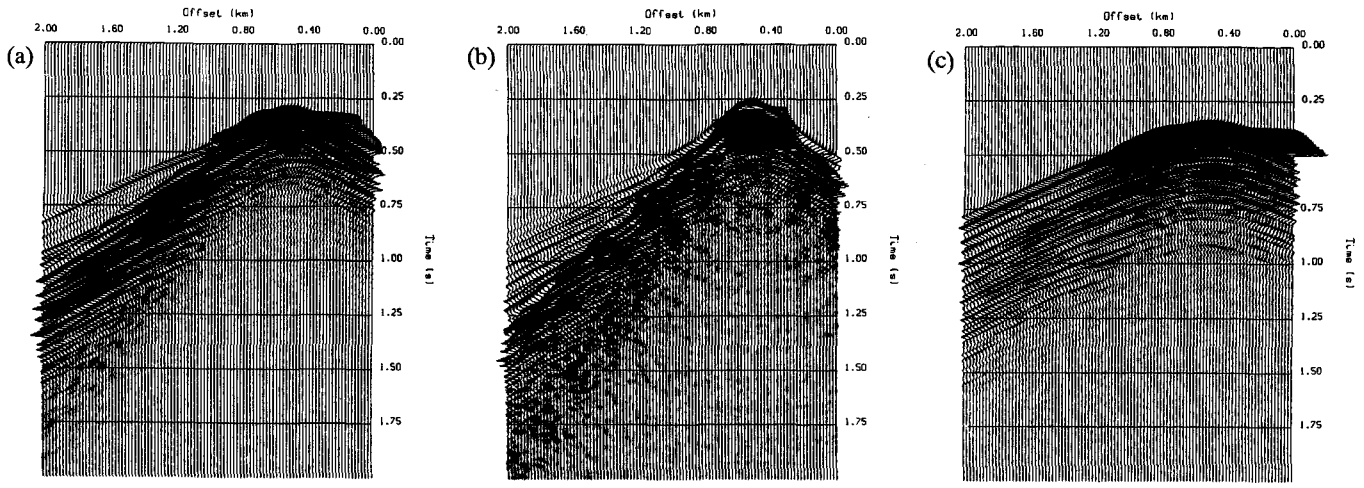

Fig. 13(a). a partial derivative seismogram with respect to the velocity of point denoted by 1 near the interface shown in Figure 2(b) a partial derivative seismogram with respect to the velocity of point denoted by 2 near the interface shown in Figure 2(c) a partial derivative seismogram with respect to the velocity of point denoted by 3 near the interface shown in Figure 2.

we consider the first arrival event regardless of the amplitude, the straight line wave event indicated by the arrow is equivalent to the straight line in Figure 12. This means that when we extract the first arrival events of the partial derivative seismograms and sum the head waves along a straight line, we can image the subsurface by using the kinematic of the partial derivative seismogram. This approach has been applied by Landa *et al.* (1993) in stacking the head waves of the field seismograms. They summed the seismic signals along a straight line and displayed the summed signal at the intercept time. Unlike the CMP reflection stacking, they stacked the seismic signal of common shot gather seismogram. The straight line of the head wave stacking by Landa *et al.* (1993) is a substitution of the stacking trial hyperbola of CMP stacking for the reflection seismograms. Since one never knows the amplitude term B and the derivative term B', one has the only choice to use the trial straight line corresponding to the kinematic approximation of the partial derivative seismogram to stack the head waves. As in CMP stacking of the reflection seismograms, one needs the static correction for the stacking of head waves using the trial straight line. With this static correction, the stacking curve for head waves is the crooked curve due to the irregular subsurface geology. In general, the stacking straight line is a good and excellent kinematic approximation of the partial derivative seismogram for the stacking of the shallow refraction data, as shown in Landa *et al.* (1993)'s experiments.

Mathematical Aspect of the Migration of the Reflection Data and the Stacking of the Refraction Data

Let us consider the summation of seismic signal along the hyperbola for the reflection seismogram (a kinematic waveform approximation of the partial derivative seismogram) or the straight line for the head waves from the mathematical point of view. The summation of seismic signal along the hyperbola can be viewed as an inner product between the field seismogram and the partial derivative seismogram, or a zero lag value of the cross correlation between the field seismogram and the partial derivative seismogram, and thus may be given as

$$\phi_i = \int_{-xmax}^{xmax} \int_0^{tmax} u(x, z=0, t) \frac{\partial u(x, z=0, \boldsymbol{p}, t)}{\partial p^i} \qquad (16)$$

where ϕ is the zero lag value of the cross correlation between the field seismogram and the partial derivative seismogram, x is the offset horizontal distance in the horizontal direction, z is the depth, t is the time, $\boldsymbol{p}$ is the parameter vector, such as velocity or density, and i denotes the ith nodal point.

It is interesting to note that the cross correlation between the field seismogram and the partial derivative seismogram tells us how much the source generated wave field (primary field) passes through the ith nodal point in the geologic media. In other words, one can measure how sensitive the field seismogram is to the ith nodal point velocity or density. One more important aspect of this inner product operation using the partial derivative seismogram lies in the similarity between the partial derivative seismogram and the Born perturbation seismogram. As discussed in the above text, the partial derivative seismogram is the seismogram generated by the virtual source. For instance, the virtual source for the computation of the partial derivative seismogram with respect to the density parameter is the product between the unit mass and the acceleration. The Born perturbation seismogram corresponds to the resulting seismogram generated by the actual source multiplied by the arbitrary small mass. Due to this affinity, the prestack depth migration tends to image the anomalous zone and the subsurface even though the initial velocity is different from the real geologic model (one wishes that the initial velocity model to be close to the real geologic model). The realities of practicing inner product operation (summation of seismic signal along the hyperbola or the straight line) in seismic data processing is that one never knows the exact partial derivative seismogram unless one uses the numerical modeling technique for the computation of the partial derivative seismogram. Even though one computes the partial derivative seismogram accurately, the application to the real data has problems in estimating the source wavelet. Without the exact source wavelet information, the inner product results in obtaining the wrong value of the zero lag value of the cross correlation. This means that if one is successful in obtaining the correct image by using the partial derivative seismogram, one has gone a step forward in solving the seismic inverse problem. A practical way of applying the partial derivative seismogram to the imaging of the subsurface is to use the kinematic waveform of the partial derivative seismogram. In considering the kinematic waveform expression of Eq. (16), we can substitute the partial derivative seismogram into the hyperbola calculated by the ray tracing or other techniques. A mathematical expression to this can be given as

$$\phi_i = \int_{-xmax}^{xmax} \int_0^{tmax} u(x, z=o, t)\, \delta\left(t - \sqrt{t_o^2 + \frac{x^2}{v^2}}\right) \qquad (17)$$

where δ is the delta function and the hyperbolic expression of the kinematic waveform of the partial derivative seismogram with respect to the material parameter.

Eq. (17) is the expression for imaging a reflection seismogram. The advantage of this kinematic approach is that when one uses the kinematic waveform of partial derivative seismogram, one excludes the multiples in calculating the inner product. Due to this, the kinematic waveform approach automatically demultiples the image of the subsurface unless the hyperbola matches the multiples, coincidently. In case of refraction waves, the hyperbola in Eq. (17) can be replaced with a straight line. The most important thing we should note is that because one never knows the amplitude term of the partial derivative seismogram when approximating it by ray tracing, one must use the amplitude term existing in the field seismogram. This is the reality faced by geophysicists in applying the Kirchhoff migration to the real seismogram.

Conclusion

A kinematic evaluation of the partial derivative seismogram, being the theoretical support for the prestack depth migration, was presented in this paper. The travel time curve calculated by ray tracing using the source and receiver reciprocity is the first arrival of the partial derivative seismograms with respect to the velocity and density. Through the analysis of the partial derivative seismograms for the acoustic wave and the elastic wave equation, the travel time curve on the basis of the acoustic media represents the first arrival of the partial derivative seismograms with respect to the P-wave velocity or the S-wave velocity or density.

For the prestack depth migration of the reflection seismogram, the summation of seismic signal along the hyperbola calculated by ray tracing results in obtaining the superimposed subsurface image of the velocity and the density. The stacking of head waves along a straight line initiated by Landa *et al.* (1993) is to use the fastest arrival travel time of the partial derivative seismogram. In this case, one discards the later wave events following the first arrival (head wave arrival) of the partial derivative seismogram. The kinematic approximation of the partial derivative seismogram by ray tracing is the fastest and the most economical tool in imaging the subsurface. However, the frequency domain modeling technique suggested by Shin and Sohn (1995) is a possible choice for future imaging technique (using the source and receiver reciprocity), giving a complete partial derivative seismogram and providing a way to compute a complete partial derivative seismogram. The full waveform imaging technique using the complete partial derivative seismogram will be a big challenge for the next generation seismic data processing, and has a possibility to reopen the floodgate to the seismic inversion frontier ed by Tarantola (1984), Chavent (1986), Mora (1987), Shin (1988), Pratt and Worthington (1990).

References

1. Bleistein, N. and Gray, S. H., 1985, An extension of the Born inversion method to a depth dependent reference profile: Geophysical Prospecting, **33**: 999-1022.
2. Gardner, G. H. F., French, W. S. and Matzuk, T., 1974, Elements of migration and velocity analysis: Geophysics, **39**: 811-825.
3. Jo, C. H., Shin, C. S. and Suh, J. H., An optimal 9 point finite difference frequency-space 2D acoustic extrapolator: Geophysics, **61**: 529-537.
4. Marfurt, K. J., 1984, Accuracy of finite difference and finite element modeling of the scalar and elastic wave equations: Geophysics, **49**: 533-537
5. Mora, P., 1987, Nonlinear two dimensional elastic inversion of multioffset seismic data: Geophysics, **52**: 1211-1228
6. Pratt, R. G. and Worthington, M. H., 1990, Inverse theory applied to multisource crosshole tomography Part 1: Acoustic wave equation method: Geophys. Prosp., **38**: 287-310.
7. Shin, C. S., 1988, Nonlinear elastic wave inversion by blocky parameterization: Ph.D thesis, University of Tulsa.
8. Shin, C. S. and Sohn, H. J., 1998, A frequency-space 2D scalar wave extrapolator using extendes 25 point finite difference operators: Geophysics, **63**.
9. Officer, C. B., 1958, Introduction to the theory of sound transmission: McGraw-hill book Company, inc.
10. Tarantola, A., 1984, Inversion of seismic reflection data in the acoustic approximation: Geophysics, **49**: 1259-1266.